Active control of composite fuselage type structures with enclosed acoustic cavity

C. Hesse[a,1,*]

[a] *Institute of Composite Structures and Adaptive Systems, German Aerospace Center (DLR), Hein-Saß-Weg 22, 21129 Hamburg, Germany*

Abstract

An active structural acoustic control system for a composite fuselage type structure is developed in this paper. The focus of the active control system is the global reduction of the sound field in an enclosed acoustic cavity using structure-integrated sensors and actuators. Active structural acoustic control systems are commonly designed based on the acoustic radiation modes which diagonalize a radiation operator. In the case of interior sound radiation, this radiation operator is derived in this paper from the coupled acoustic modes, which take into account the boundary conditions of the coupled velocity from the fuselage type structure. This results in frequency-independent radiation modes which do not rely on the validity of the modal interaction approach. The latter one violates the continuity condition of the velocity along the coupling surface. Parameter studies regarding active control implementations are conducted in order to evaluate how many radiation modes need to be considered for achieving a global sound attenuation.

Keywords: active control, ASAC, radiation modes, fluid-structure interaction

1. Introduction

Active control of structural sound radiation is an effective method to improve the low frequency acoustic insulation characteristics of lightweight aircraft structures. Especially global methods, e.g. active structural acoustic control (ASAC), offer the potential to attenuate sound in entire fluid-filled volumes like aircraft cabins, termed cavities. ASAC approaches are often concerned with the control of sound radiation from infinitely baffled plates radiating noise into the far-field [1]. For the sound radiation into cavities, cuboid cavities in contact with vibrating plates are commonly addressed [2, 3].

*Corresponding author

Email address: christian.hesse@dlr.de (C. Hesse)

[1] Present address: Institute of System Architectures in Aeronautics, German Aerospace Center (DLR), Hein-Saß-Weg 22, 21129 Hamburg, Germany

Realistic aircraft structures are formed by the circular cylindrical fuselage skin in connection with discrete frames and stringers as well as the floor. These structures are shown to exhibit a global vibrational behaviour in the low-frequency range [4, 5] where structural waves stretch over a multitude of frames and stringers. In the mid-frequency range a superposition of the global vibration modes as well as local skin segment modes occurs [6]. The high-frequency range exhibits a high modal density and the local modes are statistically distributed. However, it is shown by BIEDERMANN ET AL. [5] on the Acoustic FlightLAB demonstrator at the Zentrum für Angewandte Luftfahrtforschung (ZAL) in Hamburg that the sound radiation into the cabin is dominated by the low-frequency global fuselage modes even in the high-frequency range. This is due to the fact that these modes contain the vibrational waves with a lower wavenumber than the enclosed air and are consequently more efficient in radiating sound into the cavity.

Therefore, this paper addresses the active control of such global vibration modes of a circular cylindrical fuselage structure. For ASAC applications the structural contributions to the interior sound field are usually described in terms of the acoustic radiation modes (ARM). These are commonly calculated in order to diagonalize a radiation operator. For the interior ARMs they are derived in [7, 8] utilizing a singular value decomposition of the error weighting matrix. This formulation leads to ARMs that change with frequency and the need to sort the ARMs for each frequency step. In addition, diagonalizing the error weighting matrix which is formulated based on the uncoupled component modes can lead to eigenvalue veering over frequency, which is documented in [9, 10]. This complicates implementation on real-time signal processing, especially when modal densities are high and therefore a lot of ARMs are needed to account for the entire acoustic energy.

A formulation of the frequency-independent ARMs for circular cylindrical shells is given in [11] based on the uncoupled acoustic modes. The advantage of the frequency-independence originates from the reduced complexity for real-time implementations, which is demonstrated for the sound radiation into the far-field [12] and into cavities [3]. However, due to acoustic modes of the cylindrical cavity which contain no information, this formulation may lead to a non-intuitive implementation for the cylindrical shell. These meaningless rigid walled acoustic modes occur in [11] at a circumferential modal index of $m = 2, 4, 6, \ldots$ and radial modal index $n = 0$. Furthermore, the validity of coupling rigid-walled acoustic modes to the structure, termed modal interaction approach, is an often debated topic since the continuity condition of the velocity along the coupling surface is violated. The ARMs are therefore derived in Section 2 of this paper for a cylindrical composite test structure based on the real boundary conditions of the structural vibration on the skin surface of the cylinder rather than rigid-walled ones. The radiation efficiencies for the interior sound radiation are discussed in Section 3 as well as active control considerations using an optimal control law. Finally, Section 4 concludes this study.

2. Acoustic radiation modes

This section derives the ARMs for the composite fuselage type structure. The considered model of structural-acoustic interaction is that of a cylindrical shell coupled to an interior cylindrical cavity which is presented in Fig. 1. Since the stringers and frames change the vibrational behaviour of the structure, but only slightly affect the acoustic radiation properties into the enclosed cavity [5], they are disregarded in this study. For simplicity, the cabin floor is disregarded as well. Ultimately, this Section will derive the radiation operator, which describes the acoustic potential energy (APE) inside the cavity depending on the normal vibration of the structure.

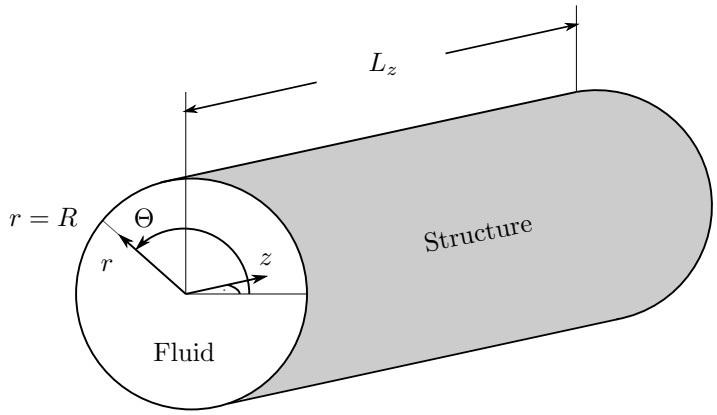

Figure 1: Cylindrical shell (grey) with interior cavity (reproduced from [11])

The problem of interior sound radiation is described in a cylindrical coordinate system with r,Θ and z describing the radial, circumferential and axial coordinates. The acoustic sound pressure $p(r, \Theta, z, \omega)$ at the position (r, Θ, z) inside the enclosure is given by the wave equation

$$\left(\nabla^2 + \kappa^2\right) p(r, \Theta, z, \omega) = 0. \tag{1}$$

Here, the wavenumber is denoted by $\kappa = \omega/c$, with the circular frequency ω and the acoustic velocity c of the medium. The Laplacian operator ∇^2 is defined in cylindrical coordinates as

$$\nabla^2 = \frac{\partial^2}{\partial r^2} + \frac{1}{r}\frac{\partial}{\partial r} + \frac{1}{r^2}\frac{\partial^2}{\partial \Theta^2} + \frac{\partial^2}{\partial z^2}. \tag{2}$$

The boundary conditions of the coupled model are given as

$$\lim_{r\to 0} p(r,\Theta,z,\omega) = p(0,\Theta,z,\omega), \tag{3}$$

$$\frac{\partial}{\partial r} p(R,\Theta,z,\omega) = -\rho i\omega v(\Theta,z,\omega), \tag{4}$$

$$p(r,\Theta,z,\omega) = p(r,\Theta+2\pi,z,\omega), \tag{5}$$

$$\frac{\partial}{\partial z} p(r,\Theta,0,\omega) = 0, \tag{6}$$

$$\frac{\partial}{\partial z} p(r,\Theta,L_z,\omega) = 0. \tag{7}$$

The pressure needs to be continuous at $r = 0$ and at $r = R$ the normal velocity is provided by the structural vibration $v(\Theta, z, \omega)$, i.e. the normal velocities of the structure and fluid are coupled. Eq. (5) describes the periodicity of the acoustic modes along the circumference while Eqs. (6) and (7) represent rigid walls at the axial positions $z = 0$ and $z = L_z$. Additional damping and absorption effects can be considered utilizing an impedance boundary condition, but are omitted here for clarity.

Using a separation of variables according to

$$p(r,\Theta,z,\omega) = p_r(r,\omega)\, p_\Theta(\Theta,\omega)\, p_z(z,\omega) \tag{8}$$

for Eq. (1) leads to the following system of differential equations

$$\left(\frac{\partial^2}{\partial z^2} + \zeta^2\right) p_z(z,\omega) = 0, \tag{9}$$

$$\left(\frac{\partial^2}{\partial \Theta^2} + \eta^2\right) p_\Theta(\Theta,\omega) = 0, \tag{10}$$

$$\left(\frac{\partial^2}{\partial r^2} + \frac{1}{r}\frac{\partial}{\partial r} + \kappa^2 - \zeta^2 - \frac{\eta^2}{r^2}\right) p_r(r,\omega) = 0, \tag{11}$$

with the additional variables ζ and η. Solving Eq. (9) with the boundary conditions Eqs. (6) and (7) leads to

$$p_z(z,\omega) = \sum_{l=0}^{\infty} A_l(\omega) \cos\left(\frac{l\pi z}{L_z}\right), \tag{12}$$

with $\zeta_l = l\pi/L_z$. Here, the axial modal index is given by $l \in \mathbb{N}_0$ with the non-negative natural numbers $\mathbb{N}_0$. The periodicity of Eq. (5) is fulfilled for the solution to Eq. (10) with integer values of $\eta = m \in \mathbb{Z}$ as

$$p_\Theta(\Theta,\omega) = \sum_{m=-\infty}^{\infty} A_\Theta(\omega)\cos(m\Theta) + B_\Theta(\omega)\sin(m\Theta). \tag{13}$$

The differential equation from Eq. (11) is solved by

$$p_r(r,\omega) = A_r(\omega) J_m\left(-i\sqrt{\zeta_l^2 - \kappa^2}\, r\right) + B_r(\omega) Y_m\left(-i\sqrt{\zeta_l^2 - \kappa^2}\, r\right) \tag{14}$$

with the bessel function of the first kind J_m and the bessel function of the second kind Y_m. Since the latter one is singular at $r = 0$, the constant B_r equals zero according to the boundary condition in Eq. (3). With the complex value $\alpha_l = \sqrt{\zeta_l^2 - \kappa^2}$, substitution of Eq. (14) in the boundary condition described by Eq. (4) leads to

$$p_{l,m}(r,\omega) = \frac{2\omega\rho v_{l,m}(\omega) J_m\left(-i\alpha_l r\right)}{\alpha_l\left(J_{m-1}\left(-i\alpha_l R\right) - J_{m+1}\left(-i\alpha_l R\right)\right)}. \tag{15}$$

Here, the contribution of structural vibration to the coupled cavity modes, denoted by the function $v_{l,m}(\omega)$, is gained from the surface integral

$$v_{l,m}(\omega) = \int_0^{2\pi}\int_0^{L_z} v(\Theta, z, \omega)\cos\left(\frac{l\pi z}{L_z}\right)\left(\cos\left(m\Theta\right) + \sin\left(m\Theta\right)\right)\mathrm{d}z\mathrm{d}\Theta. \tag{16}$$

Analogously to [11] the structural vibration are written in terms of their contribution to the ARMs $u_{l,m}(\Theta, z)$ which are independent of frequency and defined as the coupled cavity modes at the fluid-structural interface by

$$u_{l,m}(\Theta, z) = \cos\left(\frac{l\pi z}{L_z}\right)\left(\cos\left(m\Theta\right) + \sin\left(m\Theta\right)\right). \tag{17}$$

The purpose of this section is to find the time-averaged APE $E(\omega)$ depending on the structural vibration $v_{l,m}(\omega)$. The APE inside the cylindrical volume V is defined as

$$E(\omega) = \frac{1}{4\rho c^2}\int_0^R\int_0^{2\pi}\int_0^{L_z} r\left|p(r,\Theta,z,\omega)\right|^2\mathrm{d}z\mathrm{d}\Theta\mathrm{d}r. \tag{18}$$

The acoustic pressure $p(r, \Theta, z, \omega)$ is given in cylindrical coordinates as

$$p(r,\Theta,z,\omega) = \frac{1}{\pi L_z}\sum_{\substack{l=0,\\ m=-\infty}}^{\infty}\frac{1}{\epsilon_l} p_{l,m}(r,\omega)u_{l,m}(\Theta,z) \tag{19}$$

with the scalar ϵ_l defined as

$$\epsilon_l = \begin{cases} 2 & , l = 0 \\ 1 & , \text{otherwise.} \end{cases} \tag{20}$$

Due to the orthogonality condition of the coupled acoustic modes when assuming an equally distributed fluid density, each modal term of Eq. (19) can be integrated individually in Eq. (18). The APE can therefore be rewritten as

$$E(\omega) = \sum_{\substack{l=0,\\ m=-\infty}}^{\infty}\frac{\rho\omega^2 v_{l,m}(\omega)\overline{v_{l,m}}(\omega)}{c^2\pi L_z\epsilon_l\left|\alpha_l\left(J_{m-1}\left(-i\alpha_l R\right) - J_{m+1}\left(-i\alpha_l R\right)\right)\right|^2}\int_0^R r\left|J_m\left(-i\alpha_l r\right)\right|^2\mathrm{d}r, \tag{21}$$

which gives in simplified form

$$E(\omega) = \sum_{\substack{l=0,\\ m=-\infty}}^{\infty} s_{l,m}(\omega) v_{l,m}(\omega) \overline{v_{l,m}}(\omega). \tag{22}$$

Here, the operator $\overline{\{\cdot\}}$ denotes the complex conjugate of $\{\cdot\}$. With the variable $a = -i\alpha_l$, the radiation efficiency $s_{l,m}(\omega)$ of each ARM has been substituted as

$$s_{l,m}(\omega) = \frac{\rho\omega^2}{c^2 \pi L_z \epsilon_l \left|\alpha_l \left(J_{m-1}\left(aR\right) - J_{m+1}\left(aR\right)\right)\right|^2} \int_0^R r J_m\left(ar\right) J_m\left(\overline{a}r\right) \mathrm{d}r. \tag{23}$$

It should be noted, that according to the Schwarz reflection principle [13], the complex conjugate of the bessel function $\overline{J_m}\left(ar\right)$ has been rewritten as the bessel function depending on the complex conjugate of the variable a. In Eq. (23) the complex variable a defines if the integral is real or complex since the radial variable r is purely real. It is evident, that the variable a is either purely real or purely imaginary. For the case of a real a as well as non-negative m, the integral can be solved according to

$$\int_0^R r J_m\left(ar\right) J_m\left(ar\right) \mathrm{d}r = \frac{R\left(aRJ_{m-1}^2\left(aR\right) - 2mJ_{m-1}\left(aR\right) J_m\left(aR\right) + aRJ_m^2\left(aR\right)\right)}{2a}. \tag{24}$$

This includes the case of a becoming zero, which describes the cut-on frequency of an acoustic wave in z-direction. Below this cut-on frequency, for a purely imaginary a the integral can be rewritten as

$$\int_0^R r J_m\left(ar\right) J_m\left(-ar\right) \mathrm{d}r = (-1)^m \int_0^R r J_m\left(ar\right) J_m\left(ar\right) \mathrm{d}r \tag{25}$$

and solved according to Eq. (24). The integral for negative circumferential modal indices m is identical to the equivalent positive ones. Therefore an additional factor ϵ_m with

$$\epsilon_m = \begin{cases} 1 & , m = 0 \\ 2 & , \text{otherwise.} \end{cases} \tag{26}$$

is introduced in Eq. (22) as

$$E(\omega) = \sum_{\substack{l=0,\\ m=0}}^{\infty} \epsilon_m s_{l,m}(\omega) v_{l,m}(\omega) \overline{v_{l,m}}(\omega) = \sum_{\substack{l=0,\\ m=0}}^{\infty} \tilde{s}_{l,m}(\omega) v_{l,m}(\omega) \overline{v_{l,m}}(\omega). \tag{27}$$

Eq. (27) represents the interior radiation operator, which describes the APE in terms of the surrounding structural velocity. Using a numerical model of a composite fuselage type structure, the radiation efficiencies $\tilde{s}_{l,m}(\omega)$ are evaluated

in the next section. Additionally, considerations for active control implementations are described using the optimal control theory and basic excitation as well as control forces.

3. Radiation efficiencies and active control

For the studies in this paper, a finite element model of a composite test-structure is assumed. A physical representation of this test-structure is available at the DLR, which is identical to the one investigated by BIEDERMANN ET AL. [6] for the test of a new correlation criterion for model validation. This is considered a first step towards experimental investigations on ASAC systems for composite fuselage type structures. The test-structure has a length of $L_z = 2\,\mathrm{m}$, a radius of $R = 0.5\,\mathrm{m}$ and the skin is 2.2 mm thick. The shell is build from a composite lightweight material. The carbon fibre directions of the 12 layers are chosen in a way to provide a quasi-isotropic material property. The structure is made from HeyPly® M21 resign with IM7 fibres, the assumed properties of the composite material are given in Tab. 1.

Table 1: Properties of HeyPly® IM7/M21 material and composite structure

Density	$1580\,\mathrm{kg/m^3}$
Elastic properties	$E_1 = 154\,\mathrm{GPa}$; $E_2 = 8.5\,\mathrm{GPa}$; $G_{12} = 4.2\,\mathrm{GPa}$; $\nu = 0.35$
Layer thickness	0.1833 mm
Layer composition	$[60, 0, -60, 60, 0, -60, 60, 0, 60, -60, 0, 60]$
Structural damping	1 %

This section presents the finite element model as well as the calculated radiation efficiencies of the ARMs in a frequency range up to 500 Hz. A frequency increment of 1 Hz is chosen for the subsequent calculations. For the structural vibration, a frequency of 320 Hz separates the low- and high-frequency range [14] for the considered test-structure. The optimal control theory as well as active reduction of the APE and therefore a global noise attenuation are discussed.

3.1. Radiation efficiencies and model validation

This section presents the radiation efficiencies of the considered model, which rely solely on the dimensions of the cavity as well as the material constants of the contained air. For the calculations in this paper, an acoustic density of $\rho = 1.204\,\mathrm{kg/m^3}$ and a velocity of $c = 343.3\,\mathrm{m/s}$ are considered. Also the finite element model is presented and the aforementioned formulation for the APE is validated.

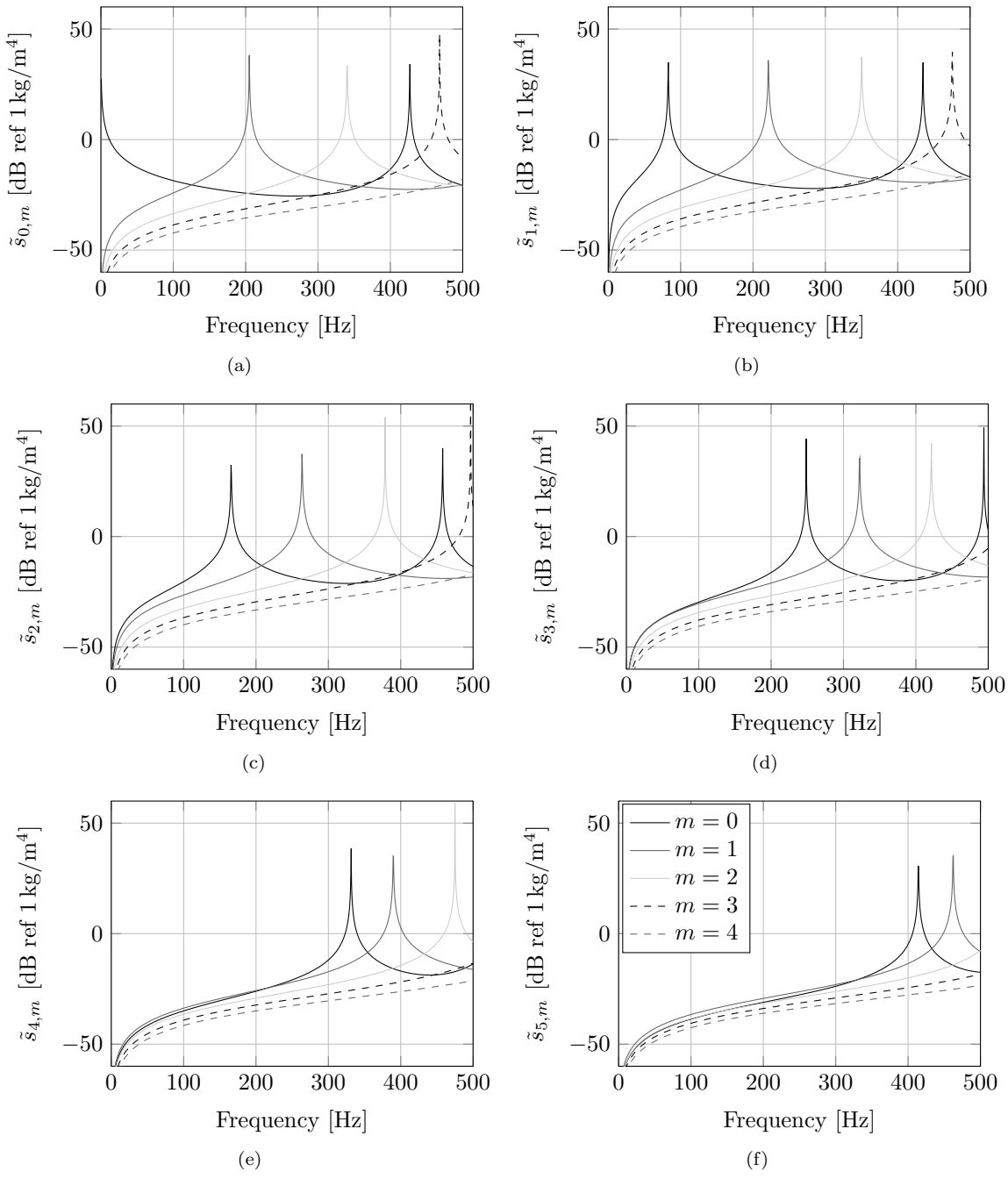

Figure 2: Overview of radiation efficiencies $\tilde{s}_{l,m}$ for the radiation modes $u_{l,m}$ with axial and circumferential modal indices l and m

The calculated radiation efficiencies $\tilde{s}_{l,m}(\omega)$ for the composite test-structure are shown in Fig. 2 depending on the modal indices (l, m) according to Eq. (27). The presented ARMs with indices $l = 0, 1, \ldots 5$ and $m = 0, 1, \ldots 4$ account for all radiation efficiencies which peak in the considered frequency regime. Due to the selective nature of the structural-acoustic coupling [15, 9], radiation modes which peak well beyond this frequency range can significantly contribute in this frequency regime. Therefore an additional number of ARMs need to be incorporated for active control of the interior sound field. The number of ARMs needed is investigated in the following sections, where the active control of a full as well as a reduced set of ARMs is considered.

The numerical model for the calculations is shown in Fig. 3, the computations are executed in Ansys®. Also depicted are the primary disturbance f_d and the control force f_c, whose positions are randomly selected. Quadratic elements of the type SHELL281 are used for the structure and FLUID220 for the fluid. Both ends of the cylinder are assumed to be simply supported for the numerical calculations. According to Eq. (16) the structural velocity $v(\Theta, z, \omega)$ can be understood as an excitation of the internal cavity modes. Therefore the type of structural boundary conditions does not impair the validity of the aforementioned formulation. This is also the case for anisotropic material properties of the composite structure.

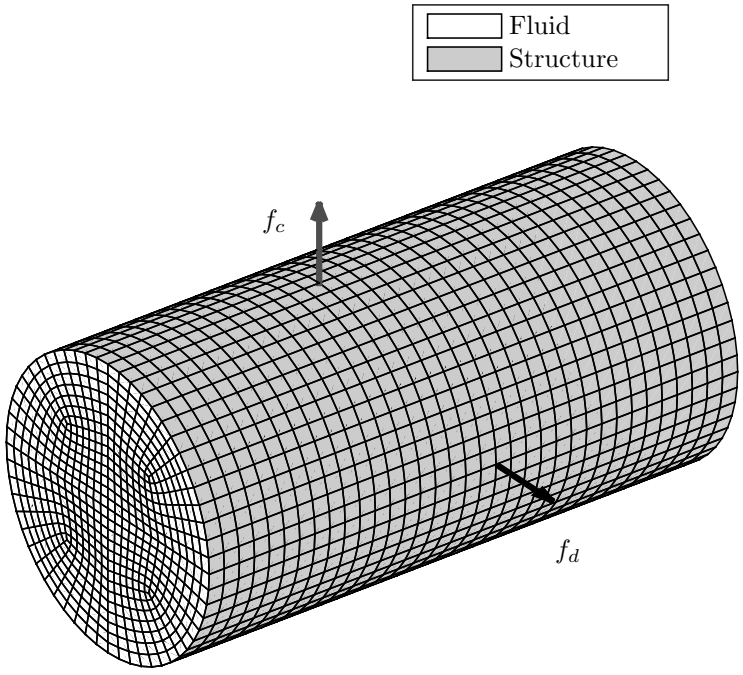

Figure 3: Finite element model of cylindrical shell with interior cavity

In order to validate the approach described in Section 2, the APE for the nu-

merical model is estimated and compared to the analytical formulation. This is done through numerical integration of the pressure values according to Eq. (18). As a reference value, the pressure values are extracted from a harmonic analysis in Ansys®with only the disturbance excitation f_d. This value is compared to the one estimated along the structural surface according to Eq. (27). For this analytical evaluation ARMs with modal indices of $l = 0, 1, \ldots, 10$ and $m = 0, 1, \ldots, 15$ are considered. The coupled response of the structural velocity as calculated in Ansys®is integrated along the structural surface according to Eq. (16) Comparing the resulting APE in Fig. 4, a good agreement is evident. The relative deviation magnitude amounts to 0.86 %, averaged over frequency.

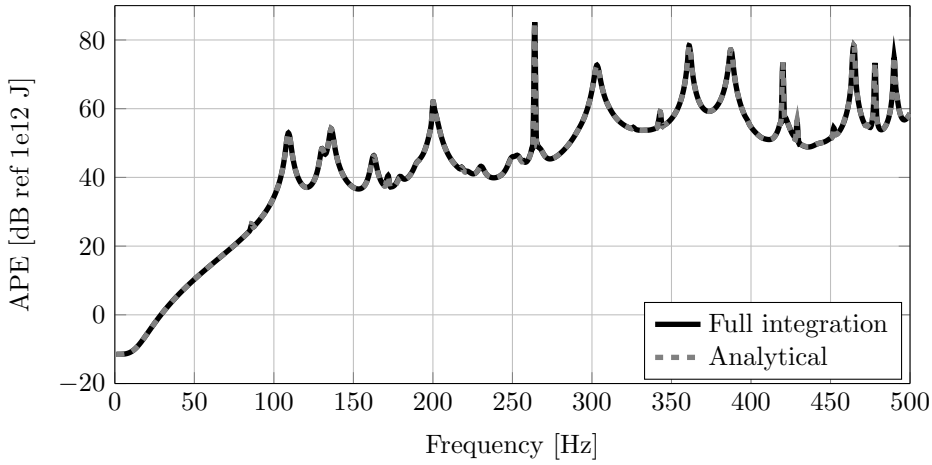

Figure 4: Comparison of APE for different integration methods

The following section describes the optimal control theory which is subsequently used for the active control considerations of the APE in the enclosed acoustic cavity.

3.2. Optimal control

For the active control considerations an optimal control system is assumed, a detailed description of which can be found in [16]. This is an idealised control system, which can describe an upper limit on what an active controller can achieve. It should be noted, that in real-time applications using a feedforward controller these reductions are not representative for broadband, stochastic excitations. This is due to causality constraints and coherence restrictions which degrade the optimal controller, as described in detail in [17]. However, for deterministic, narrowband excitations they can give a reliable estimate of the achievable reduction.

When assuming the system to be linear and in steady state, the normal structural vibration $\mathbf{v}$ can be written as superposition of the disturbance path $\mathbf{h}_d$ and the control path $\mathbf{h}_c$ as

$$\mathbf{v} = \mathbf{h}_d f_d + \mathbf{h}_c f_c. \tag{28}$$

Here, the scalars f_d and f_c describe the disturbance and control input, respectively. The frequency-dependence of $\mathbf{v}$ has been omitted for the purpose of brevity. The aim of the optimal control synthesis is to find a control input f_c which minimises a quadratic error criterion

$$J = \mathbf{v}^H \mathbf{S} \mathbf{v}. \tag{29}$$

The diagonal matrix $\mathbf{S}$ contains the radiation efficiencies $\tilde{s}_{l,m}$ on its main diagonal analogously to Eq. (27). Provided that $\mathbf{h}_c^H \mathbf{S} \mathbf{h}_c$ is not singular, this quadratic error criterion is minimised by

$$f_{c,min} = -\left(\mathbf{h}_c^H \mathbf{S} \mathbf{h}_c\right)^{-1} \mathbf{h}_c^H \mathbf{S} \mathbf{h}_d f_d. \tag{30}$$

The optimal control theory is applied in the next section to the active noise reduction of the enclosed sound field.

3.3. Control results

It was discussed in Section 3.1, that ARMs whose radiation efficiencies peak beyond the frequency range of interest can contribute to the interior APE. The number of ARMs necessary to account for the major part of the APE therefore needs to be known before the control synthesis in order to get a proper reduction. Therefore a measure is proposed in this section, which allows the evaluation of ARMs needed. The results of the optimal control synthesis are presented in this section for different configurations and the consistency of the reductions to the considered ARMs is shown.

To estimate the number of ARMs needed, a measure $\sigma_{l,m}$ is proposed as

$$\sigma_{l,m} = \int_{f_{min}}^{f_{max}} \left| v_{l,m}(\omega) \right|^2 \mathrm{d}f \tag{31}$$

dependent on the structural vibration contributions to the ARMs integrated over the frequency range of interest. The measure $\sigma_{l,m}$ is presented for the composite test structure in Fig. 5. The low-order ARMs clearly contribute the most to the internal APE inside the enclosed cavity. The most dominant modes are the ones with an axial modal index of $l = 0$. Modes with a circumferential modal index of $m < 2$ and $m > 14$ do not contribute significantly.

The circumferential and axial wavenumber increase with frequency to a different extent. Since the circumference is bigger than the axial length for the considered test-structure, the circumferential wavenumber increases faster than the axial one. Therefore, ARMs with higher circumferential modal indices m need to be considered than axial indices l for the APE evaluation and subsequent active control considerations.

For the active control synthesis, three different sets of ARMs are considered. A full set $\mathbb{P}_{\text{full}}$ includes all ARMs used for the evaluation of the APE in Fig. 4, this includes the ARMs with modal indices of $l = 0, 1, \ldots, 10$ and

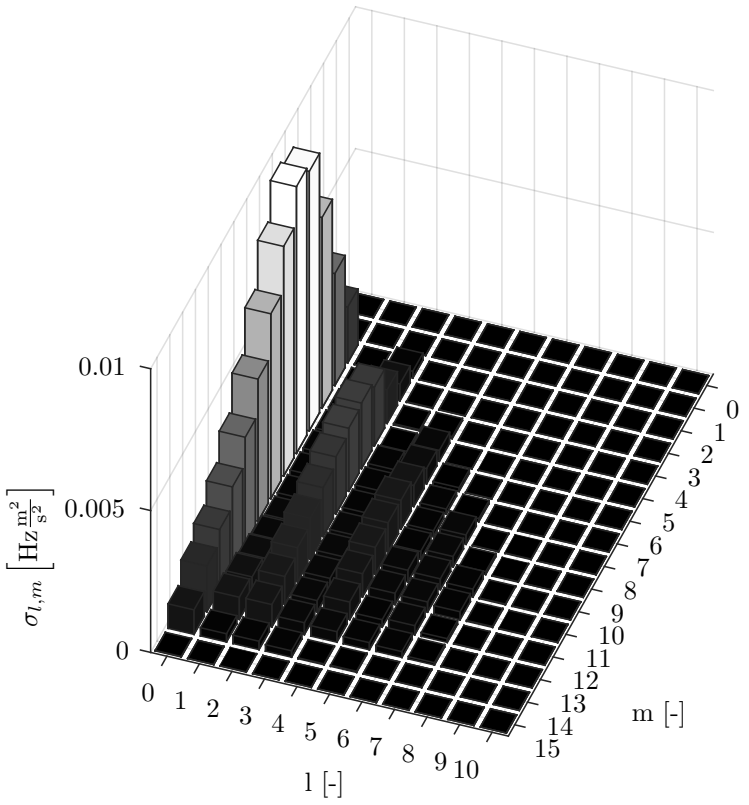

Figure 5: Contribution estimate $\sigma_{l,m}$ to the ARMs

$m = 0, 1, \ldots, 15$. A reduced set $\mathbb{P}_{\mathrm{red},1}$ includes the ARMs with modal indices of $l = 0, 1, \ldots, 4$ and $m = 2, \ldots, 14$, as these include most contribution to the interior APE. A second reduced set $\mathbb{P}_{\mathrm{red},2}$ includes the ARMs with modal indices of $l = 0$ and $m = 2, \ldots, 14$.

Table 2: Mean APE for different number of ARMs considered for active control

Concept	APE
No control	43.08 dB
Control $\mathbb{P}_{\mathrm{full}}$	37.98 dB
Control $\mathbb{P}_{\mathrm{red},1}$	38.44 dB
Control $\mathbb{P}_{\mathrm{red},2}$	41.33 dB

The mean APE reductions over frequency are given in Tab. 2. The APE reduction for discrete frequencies is shown in Fig. (6). The consideration of a full set $\mathbb{P}_{\mathrm{full}}$ of ARMs for active control leads to a global reduction of 5.10 dB in APE averaged over frequency. In discrete frequencies it can be seen, that nearly all peaks are reduced. The peaks unaltered are due to the control force

placed near the line of nodes for the operational deflection shapes rather than a deficit of ARMs. Considerable global reductions of 4.64 dB can still be achieved by the reduced set $\mathbb{P}_{\text{red},1}$ of ARMs. This substantiates the effectiveness of the measure $\sigma_{l,m}$ in determining the number of ARMs necessary for active control considerations.

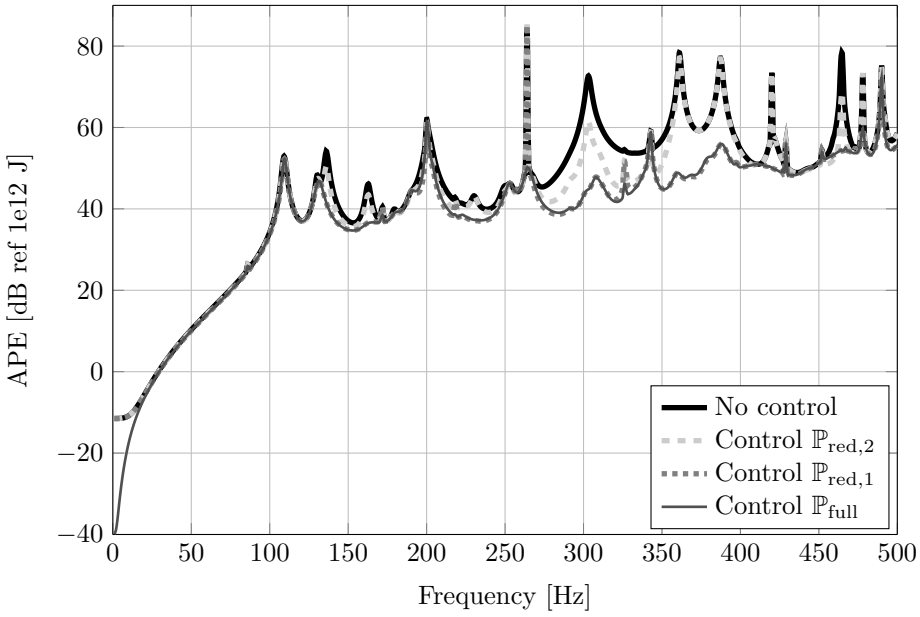

Figure 6: Control results

As expected, the reduced set $\mathbb{P}_{\text{red},2}$ leads to a decrease in control performance with 1.75 dB reduction averaged over frequency. However, the implementation effort is also less with a total of 13 ARMs considered compared to 65 and 176 for $\mathbb{P}_{\text{red},1}$ and $\mathbb{P}_{\text{full}}$, respectively. The inability of the reduced control configurations $\mathbb{P}_{\text{red},1}$ and $\mathbb{P}_{\text{red},2}$ to control the peak at 264 Hz is due to the omission of the radiation efficiency $\tilde{s}_{2,1}$ which peaks near this frequency according to Fig. 2c. Although the contribution estimate $\sigma_{2,1}$ is low, the ARM can still contribute significantly in narrow frequency bandwidths.

4. Conclusion

This study addresses the active control of composite fuselage type structures where the focus is the reduction of noise inside the enclosed acoustic cavity. Specifically, a global reduction inside the cavity is targeted by use of structure-integrated sensors and actuators. Therefore the ARMs are derived in a form, that they are independent of frequency and as a result are easily implemented in active control systems. This novel formulation is achieved by considering the structural velocity as boundary condition to the interior cavity modes. The

described formulation is therefore robust to structural anisotropies and arbitrary damping distributions as well as independent of the type of structural boundary conditions. Furthermore, the described formulation is not dependent on the validity of the modal interaction approach since the velocity condition on the coupling surface is retained. A contribution estimate has been introduced in order to evaluate the number of ARMs necessary to account for the interior acoustic energy. Using an optimal control law and considering different subsets of ARMs, the contribution estimate was shown to reliably identify the dominant contributors to the frequency averaged APE. In narrow frequency bands slight deviations may occur in the vicinity of acoustic resonances.

A physical model of the composite structure has been build at the DLR and experimental studies regarding global noise reduction will be executed in future investigations. The necessary numbers of ARMs obtained from this study will be further utilized for experimental control exploration.

References

[1] S. J. Elliott, M. E. Johnson, Radiation modes and the active control of sound power, The Journal of the Acoustical Society of America 94 (1993) 2194–2204.

[2] A. K. Bagha, S. V. Modak, Active structural-acoustic control of interior noise in a vibro-acoustic cavity incorporating system identification, Journal of Low Frequency Noise, Vibration and Active Control 0 (2017) 1–16.

[3] C. Hesse, V. Papantoni, S. Algermissen, H. P. Monner, Frequency-independent radiation modes of interior sound radiation: Experimental study and global active control, Journal of Sound and Vibration 401 (2017) 204–213.
URL `http://elib.dlr.de/112117/`

[4] P. C. Herdic, B. H. Houston, M. H. Marcus, E. G. Williams, A. M. Baz, The vibro-acoustic response and analysis of a full-scale aircraft fuselage section for interior noise reduction, The Journal of the Acoustical Society of America 117 (6) (2005) 3667–3678.

[5] J. Biedermann, R. Winter, M. Norambuena, M. Böswald, M. Wandel, Classification of the mid-frequency range based on spatial fourier decomposition of operational deflection shapes, in: 24th International Congress on Sound and Vibration, 2017.

[6] J. Biedermann, R. Winter, M. Wandel, M. Böswald, Energy based correlation criteria in the mid-frequency range, Journal of Sound and Vibration 400 (2017) 457–480.

[7] B. S. Cazzolato, C. H. Hansen, Active control of sound transmission using structural error sensing, The Journal of the Acoustical Society of America 104 (1998) 2878–2889.

[8] W. M. Johnson, K. A. Cunefare, Use of principle velocity patterns in the analysis of structural acoustic optimization, The Journal of the Acoustical Society of America 121 (2) (2007) 938–948.

[9] C. Hesse, Aktive Reduktion der Schalleinstrahlung in Kavitäten, Ph.D. thesis, Deutsches Zentrum für Luft-und Raumfahrt e.V. (2016).
URL http://elib.dlr.de/111817/

[10] R. Davis, A simplified approach for predicting interaction between flexible structures and acoustic enclosures, Journal of Fluids and Structures 70 (2017) 276–294.

[11] C. Hesse, J. M. V. Perez, M. Sinapius, Frequency-independent radiation modes of interior sound radiation: An analytical study, Journal of Sound and Vibration 392 (2017) 31–40.
URL http://elib.dlr.de/111808/

[12] G. P. Gibbs, R. L. Clark, D. E. Cox, J. S. Vipperman, Radiation modal expansion: Application to active structural acoustic control, The Journal of the Acoustical Society of America 107 (1) (2000) 332–339.

[13] I. N. Bronstein, K. A. Semendjajew, G. Musiol, H. Mühlig, Taschenbuch der Mathematik, 5th Edition, Verlag Harri Deutsch, Frankfurt/Main, 2001.

[14] J. Biedermann, Energiebasierte Korrelation von strukturdynamischen Messungen mit numerischen Modellen für Strukturen mit hoher modaler Dichte, Ph.D. thesis, Deutsches Zentrum für Luft-und Raumfahrt e.V. (2016).
URL http://elib.dlr.de/105430/

[15] S. Snyder, C. Hansen, The design of systems to control actively periodic sound transmission into enclosed spaces, part ii: mechanisms and trends, Journal of sound and vibration 170 (4) (1994) 451–472.

[16] M. H. H. Oude Nijhuis, Analysis tools for the design of active structural acoustic control systems, Ph.D. thesis, University of Twente, Enschede, The Netherlands (2003).

[17] M. Misol, Aktive Steuerung des Transmissionsverhaltens stochastischer Störquellen durch flächige Leichtbaustrukturen, Ph.D. thesis, Deutsches Zentrum für Luft-und Raumfahrt e.V. (2014).
URL http://elib.dlr.de/99510/